Skeletal Radiol (2017) 46:1695–1706
DOI 10.1007/s00256-017-2739-x

SCIENTIFIC ARTICLE

High-resolution 3-T MRI of the triangular fibrocartilage complex in the wrist: injury pattern and MR features

Huili Zhan[1] · Huibo Zhang[2] · Rongjie Bai[1,3] · Zhanhua Qian[1,3] · Yue Liu[1] · Heng Zhang[1] · Yuming Yin[4]

Received: 6 January 2017 / Revised: 17 July 2017 / Accepted: 20 July 2017 / Published online: 15 August 2017

Abstract
Objectives To investigate if using high-resolution 3-T MRI can identify additional injuries of the triangular fibrocartilage complex (TFCC) beyond the Palmer classification.
Materials and methods Eighty-six patients with surgically proven TFCC injury were included in this study. All patients underwent high-resolution 3-T MRI of the injured wrist. The MR imaging features of TFCC were analyzed according to the Palmer classification.
Results According to the Palmer classification, 69 patients could be classified as having Palmer injuries (52 had traumatic tears and 17 had degenerative tears). There were 17 patients whose injuries could not be classified according to the Palmer classification: 13 had volar or dorsal capsular TFC detachment and 4 had a horizontal tear of the articular disk.
Conclusion Using high-resolution 3-T MRI, we have not only found all the TFCC injuries described in the Palmer classification, additional injury types were found in this study, including horizontal tear of the TFC and capsular TFC detachment. We propose the modified Palmer classification and add the injury types that were not included in the original Palmer classification.

Keywords Wrist · Triangular fibrocartilage complex · Injury · Magnetic resonance imaging

Rongjie Bai and Yuming Yin contributed equally to this work

✉ Rongjie Bai
bairongjie@126.com

[1] Department of Radiology, Peking University Fourth School of Clinical Medicine, No.31, Xinjiekou East Street, Xicheng District, Beijing 100035, China

[2] Department of Radiology, Beijing Chaoyang Hospital of Capital Medical University, No. 8, Gongti South Road, Chaoyang District, Beijing 100020, China

[3] Department of Radiology, Beijing Jishuitan Hospital, Beijing Institute of Traumatology and Orthopedics, No.31, Xinjiekou East Street, Xicheng District, Beijing 100035, China

[4] Radiology Associates, LLP, 1814 South Alameda Street, Corpus Christi, TX 78404, USA

Introduction

Triangular fibrocartilage complex (TFCC) is composed of triangular fibrocartilage (TFC, the articular disk), meniscal homolog (MH), dorsal and volar distal radioulnar ligaments, the extensor carpi ulnaris tendon (ECU), ulnocarpal collateral ligament (UCL), and ulnotriquetral (UT) and ulnolunate (UL) ligaments. The TFCC is the main stabilizer of the ulnar-sided wrist and the distal radioulnar joint (DRUJ). It plays a significant role in wrist biomechanics and can dissolve and absorb the force transmitted between the ulna and ulnar side of the carpal bones. It plays an important role in maintaining the stability of the ulnocarpal joint and allows the stable motion of the distal radioulnar joint during the rotation of the forearm [1–7]. Injury to one or more of the TFCC components may cause ulnar-sided wrist pain and may lead to wrist instability.

Magnetic resonance imaging (MRI) can yield a high-resolution image of soft tissue and visualize the detailed anatomical structures of the TFCC. MRI, especially the high-resolution 3-T MRI has been regarded as the preferred imaging modality in the evaluation of TFCC injuries [8–13]. In 1989, based on the cause, location, and extent of TFCC injuries, Palmer successfully introduced a classification system for TFCC injuries, which has been widely used and is critical in selecting the treatment options [14]. With the advanced 3-T

Table 1 Palmer classification of triangular fibrocartilage complex (TFCC) lesions

Class I lesions (traumatic)	Class II lesions (degenerative)
IA. Central perforation	IIA. TFC wear
IB. Ulnar avulsion	IIB. TFC wear with chondromalacia
IC. Distal avulsion	IIC. TFC perforation with chondromalacia
ID. Radial avulsion	IID. TFC perforation, chondromalacia, and lunotriquetral ligament perforation
	IIE. TFC perforation, chondromalacia, lunotriquetral ligament perforation, and ulnocarpal/radioulnar arthritis

MR scanner available, we have found more injury types that were not covered by the original Palmer classification.

This research was designed to study if the Palmer classification could include all the different injury patterns found on high-resolution 3-T MR and investigate their MRI features in surgically proven cases of TFCC injuries.

Materials and methods

This research protocol was reviewed and approved by our institutional ethics review board. Informed consent was obtained from all individual participants included in the study.

Table 2 The modified Palmer classification of TFCC lesions

Class I lesions (traumatic)	Class II lesions (degenerative)
IA. Central perforation of the TFC	IIA. TFC wear
IB. Ulnar avulsion of the TFC	IIB. TFC wear with chondromalacia
IC. Distal avulsion of the ulnotriquetral and ulnolunate ligaments	IIC. TFC perforation with chondromalacia
ID. Radial avulsion of the TFC	IID. TFC perforation, chondromalacia, and lunotriquetral ligament rupture
IE. Horizontal tear of the articular disk	IIE. TFC perforation, chondromalacia, lunotriquetral ligament perforation, and ulnocarpal/radioulnar arthritis
IF. Volar capsular TFC detachment	
IG. Dorsal capsular TFC detachment	
IH. Dorsal capsule detachment from the triquetral insertion	
II. Dorsal capsular TFC detachment and detachment from the triquetral insertion	

TFC triangular fibrocartilage

Subjects

Eighty-six patients with ulnar-sided wrist pain who had confirmed TFCC injuries by surgery between March 2014 and March 2016 were included and analyzed in this study.

Inclusion criteria

To be included in this study, all patients with surgically proven TFCC injuries had to have initially presented with ulnar-sided wrist pain. The clinical history was learned by reviewing the patient's charts and interviewing the patients.

Exclusion criteria

The patients who had inflammatory arthritis, tumor or tumor-like lesions, deformity of the wrist (such as Madelung deformity), or post-orthopedic surgery involving the hand, wrist, and distal forearm other than TFC repair were excluded from this study.

Magnetic resonance imaging

Magnetic resonance examination was performed using a 3-T MRI unit (Philips Achieva; Philips Medical Systems, Best, The Netherlands) with a 16-channel hand-and-wrist receiver-only coil (Philips Hand/Wrist 16 3 T Tim coil, model (IT)).

The patients were placed in prone position and the examined arms were raised above the head, with the wrist in neutral position in the magnetic isocenter pinpointed by the laser mark. All patients underwent magnetic resonance examination with the following sequences: proton density fat-suppressed (PD FS) imaging in axial, coronal, and sagittal planes (TR/TE 2,347–3,657/40–45), and T1-weighted fast spin-echo in the coronal plane (TR/TE 521–780/20–40), slice thickness was 2 mm, with an interslice space of 0.3 mm, NEX 2–4, field of view 100–120 mm, and voxel (0.15–0.25) mm*(0.15–0.25)mm*1.50 mm.

Magnetic resonance imaging analysis

All MR images were interpreted independently by two musculoskeletal radiologists who had 5 and 10 years' experience. Both radiologists were blinded to the clinical data, including the findings in the surgery reports. The discrepancies were resolved by consensus by introducing an additional musculoskeletal radiologist with more than 10 years' experience. The appearance of TFCC and signal intensity on MR images of the 86 patients with surgically proven TFCC injuries were analyzed based on the Palmer classification. The MRI features of different subtypes of the injuries were compared with the surgical results in a double-blind manner.

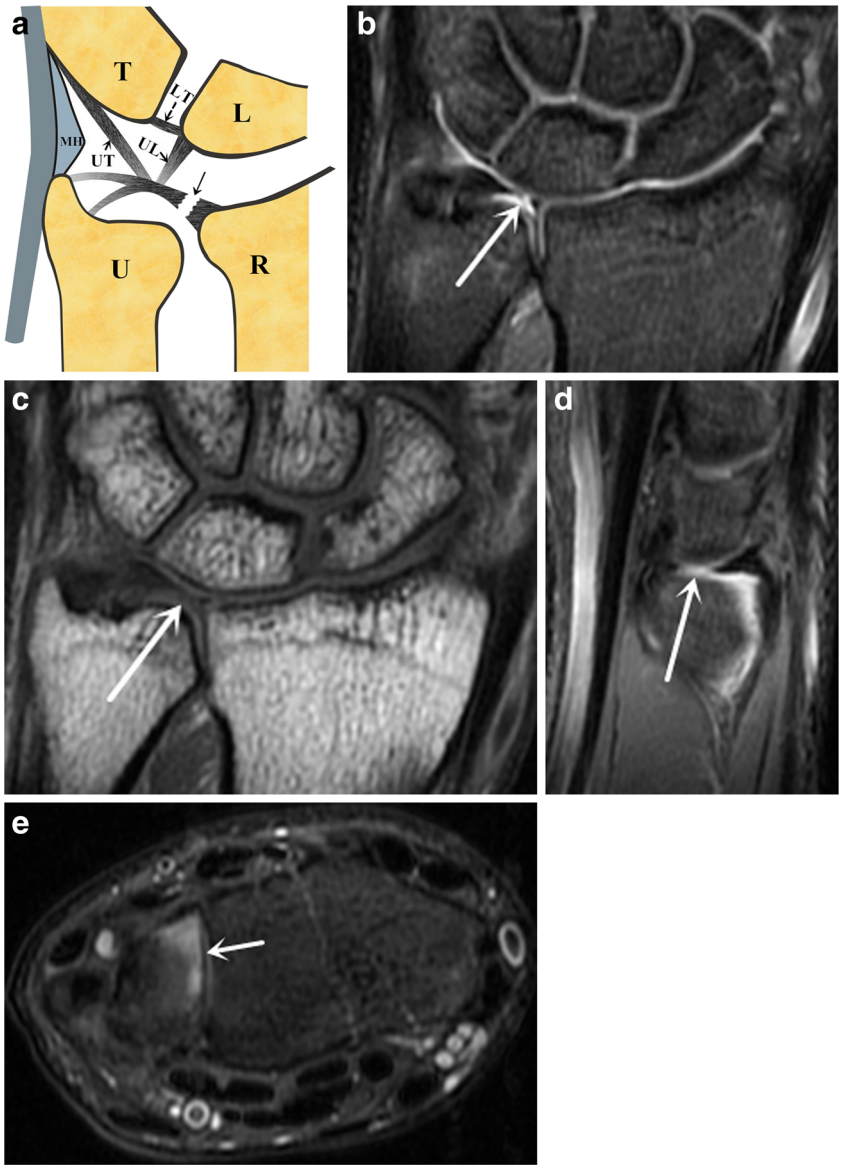

Fig. 1 Class IA: central perforation. **a** Schematic drawing of Palmer IA injury showed the central tear of the triangular fibrocartilage (TFC) disc (*arrow*). *LT* lunotriquetral ligament, *UL* ulnolunate ligament, *UT* ulnotriquetral ligament, *MH* meniscal homolog, *R* radius, *U* ulna, *L* lunate, *T* triquetrum. **b–e** A 28-year-old man with a wrist injury. **b** Coronal proton density fat-suppressed (PD FS) image showed high signal intensity near the radial attachment of the TFC (*white arrow*) and fluid high signal intensity in the distal radioulnar joint (DRUJ). **c** Coronal T1-weighted image showed that the focal structures of the triangular fibrocartilage complex (TFCC) were obscured (*white arrow*). **d** Sagittal PD FS weighted image showed a slit-like area of high signal intensity (*white arrow*) in the normal biconcave low signal TFC. **e** Axial PD FS weighted image of the wrist showed that the high PD signal intensity traveled in the sagittal direction (*white arrow*)

Results

TFCC injuries on MRI

The diagnosis of traumatic or degenerative injuries depended on a combination of factors, including the clinical history, the patient's age, the location of injuries, and the associated injuries. Among 86 patients with surgically proven TFCC injuries, 69 injury patterns could be classified using the Palmer classification (Table 1). There were 17 TFCC injuries that could not be classified by the Palmer classification. Table 2 lists the detailed classification of injuries of the TFCC that we suggested.

Among the 69 Palmer injury patterns, there were 52 patients with traumatic TFCC injuries including 23 men, 29 women, with ages ranging from 15 to 68 years and an average age of 37 years. There were 17 patients with degenerative TFCC injuries including 5 men, 12 women, and an age range of 22–79 years, with an average age of 50 years.

The 52 traumatic injuries included the following: IA (central perforation of the TFC) = 9, IB (ulnar avulsion of the TFC) = 25, IC (distal avulsion of the ulnotriquetral and ulnolunate ligaments) = 3, ID (radial avulsion of the TFC) = 13, compound injury = 2.

In class IB injuries, in addition to the ulnar avulsion of the TFC, 1 patient also had avulsion of the ulnar styloid and fracture of the distal radius simultaneously. In the class IC injuries, in addition to the distal avulsion of the ulnotriquetral and ulnolunate ligaments, 1 patient also had a Colles fracture and the other one had injuries of multiple ligaments (including the scapholunate ligament and lunotriquetral ligament). In class ID injuries, in addition to radial avulsion of the TFC, 1

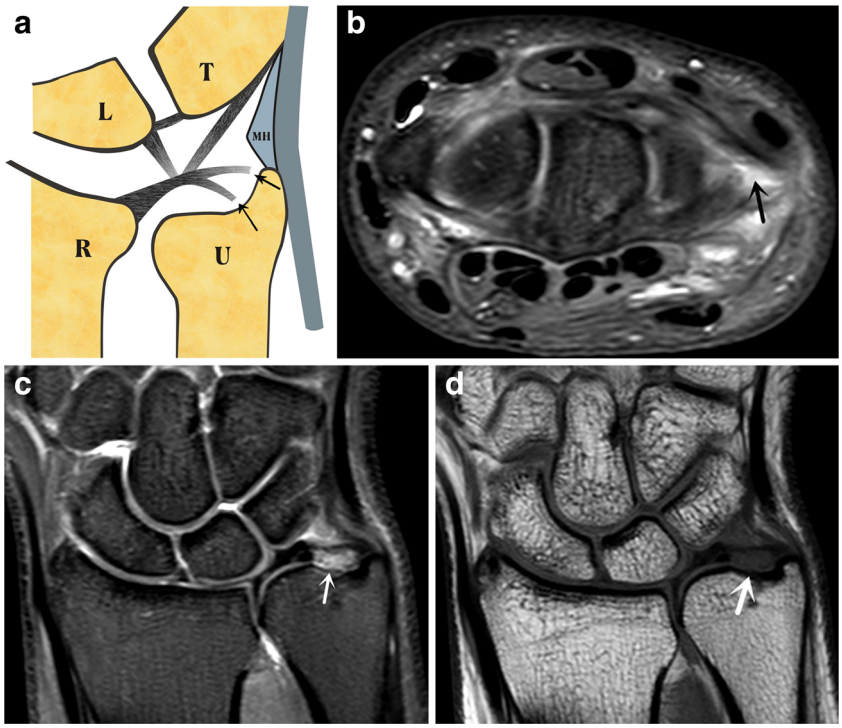

Fig. 2 Class IB: ulnar avulsion. **a** Illustration drawing of Palmer IB injury showing the ulnar side rupture (*arrow*). **b–d** A 37-year-old man with a wrist injury. **b** axial, **c** coronal PD FS images and **d** coronal T1-weighted image of the wrist showed the ulnar side rupture, which presented as irregular high signal intensity in the ulnar attachment of TFC (*arrow*)

patient also showed a fracture at the distal-most aspect of the sigmoid notch of the radius.

Among the compound traumatic TFCC injuries, 1 patient showed central perforation with avulsion of the ulnar attachment. The other one had ulnar and radial injuries.

The diagnosis of degenerative tear mainly depended on the lack of traumatic history, the location of abnormal findings, and the associated degenerative changes in the adjacent structures. The associated degenerative changes of the adjacent structures include thinning of the articular cartilage along the ulnar side of the proximal lunate and/or the adjacent triquetrum, the presence of a subchondral cyst or subchondral sclerosis of the proximal ulnar side of the lunate and/or the radial side of the proximal triquetrum, thinning of the articular cartilage of the distal ulna, subchondral cyst formation or increased subchondral sclerosis of the distal ulna, and tear of the lunotriquetral ligament.

Among the 17 degenerative injuries: IIA (TFC wear) = 5, IIB (TFC wear with chondromalacia) = 2, IIC (TFC perforation with chondromalacia) = 2, IID (TFC perforation, chondromalacia, and lunotriquetral ligament rupture) = 2, IIE (TFC perforation, chondromalacia, lunotriquetral ligament perforation, and ulnocarpal/radioulnar arthritis) = 6.

There were 17 TFCC injuries that could not be classified according to the Palmer classification criteria, 8 patients had detachment of the dorsal joint capsule from the TFC, 4 patients had a horizontal tear of the articular disk, 3 patients had distal detachment of the dorsal capsule in its insertion into the dorsal side of the triquetrum, 1 patient had detachment of the volar joint capsule from the TFC, and 1 patient had dorsal capsule detachment in the insertion and in the dorsal edge of triquetrum. These 17 patients consisted of 7 men, 10 women, and had an age range of 15–68 years, with average age of 37 years.

Palmer classification of TFCC injuries and MR imaging

Class I lesions (traumatic)

Class IA indicated perforation of the articular disk of the TFCC or central tear of the TFC, and was found in 9 patients (Fig. 1). On PD FS images, central perforation could be well recognized, shown as linear hypersignal intensity within the low-signal TFC. On the sagittal plane, the high signal intensity traveled from the volar to the dorsal side. In addition, this type of perforation could be accompanied by joint effusion in the distal radioulnar joint, whereas the other structures of TFCC may be normal (Fig. 1).

Class IB indicated ulnar avulsion of the TFC and was found in 25 patients. The attachments of the triangular ligament to the ulnar styloid and the ulnar fovea were injured (Fig. 2). On MR images, the TFC ulnar attachment showed discontinuity of the triangular ligament with irregular hypersignal intensity between the central disc and the ulnar styloid. The lesion could be best appreciated on coronal PD FS images (Fig. 2). Among patients with type IB lesions, 1 patient also had both avulsion fracture of the ulnar styloid and fracture of the distal radius.

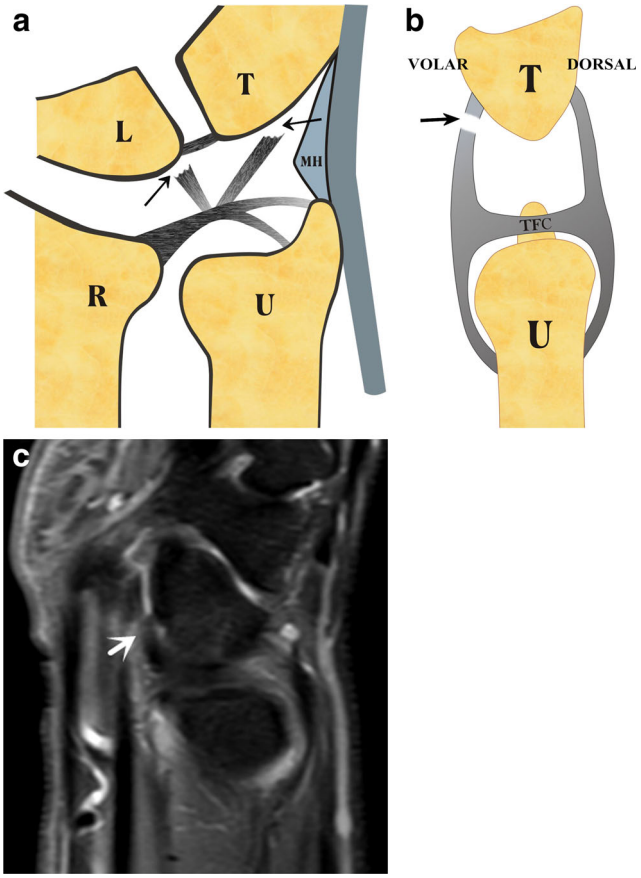

Fig. 3 Class IC: distal avulsion. **a**, **b** Schematic drawing of Palmer IC injuries showed tear of the ulnocarpal ligaments including the ulnolunate ligament and ulnotriquetral ligament, which was not related to the capsule (*arrow*). **c** A 54-year-old woman with a wrist injury. Sagittal PD FS image of the wrist showed the discontinuity of the ulnotriquetral ligament with high signal intensity filling in the gap (*arrow*)

Class IC indicated distal avulsion of the ulnotriquetral and ulnolunate ligaments and was found in 3 patients. It was characterized by the discontinuity of the ulnotriquetral and ulnolunate ligaments (Fig. 3). On MR images, the ulnotriquetral and the ulnolunate ligament tears were best shown on sagittal PD FS images (Fig. 3). One patient had a Colles fracture whereas the other had fractures of the scaphoid and triquetrum with intrinsic ligament injuries including the scapholunate ligament and lunotriquetral ligament.

Class ID indicated radial avulsion of the TFC and was found in 13 patients. It involved the separation of the radial side attachment of the TFC from the sigmoid notch of the distal radius and showed the irregular linear hypersignal intensity between the radial side of the TFC and the sigmoid notch, best seen on coronal PD FS images (Fig. 4). One patient had a fracture in the distal radius. There were 2 patients with a traumatic pattern who were misinterpreted as having central perforation on the MR images by both reviewers, whereas the surgical result was proven to be the radial avulsion (Fig. 5).

Class II lesions (degenerative)

Class IIA indicated TFC wear and was found in 5 patients. In this group, the TFC underwent degenerative wear and underwent focal thinning with surface abrasion, but remained intact (Fig. 6). On MR images, this lesion showed increased signal intensity within the low signal TFC with the loss of a sharp margin of both the superior and the inferior surface on T1-weighted and PD FS images (Fig. 6).

Class IIB indicated TFC wear with chondromalacia and was found in 2 patients. Palmer IIB injuries included changes in Palmer IIA and cartilage changes on the proximal ulnar aspect of the lunate or radial portion of the distal ulna (Fig. 7). On MR images, in addition to showing the thinning of the TFC with intermediate signal intensity, more advanced than in IIA, thinning of the articular cartilage along the ulnar side of the proximal lunate and radial side of the proximal triquetrum was also shown. These changes may be associated with adjacent bone marrow edema and subchondral cyst formation in the adjacent lunate and the triquetrum (Fig. 7).

Class IIC indicated TFC perforation with chondromalacia and was found in 2 patients. This group was characterized by severe thinning of the TFC with severe perforation (Fig. 8). On MR images, there was a large defect in the center of the TFC with diffuse hypersignal intensity of the TFC. This is different from the slit-like area of high signal intensity in class IA lesions. The adjacent lunate showed bone marrow edema with a subchondral cyst on PD FS images (Fig. 8).

Class IID indicated TFC perforation, chondromalacia, and lunotriquetral ligament rupture and was found in 2 patients. This group of patients had degenerative tear of the TFC, loss of articular cartilage of the lunate with subchondral bone marrow edema, and tear of the lunotriquetral ligament. On MR images, there was a complete tear of the TFC, which became irregular with increased signal intensity, thinning or complete loss of the articular cartilage along the ulnar side of the proximal lunate with hypersignal intensity within the ulnar proximal side of the lunate. The lunotriquetral ligament was absent on the PD FS image (Fig. 9).

Class IIE indicated TFC perforation, chondromalacia, lunotriquetral ligament perforation, and ulnocarpal/radioulnar arthritis and was found in 6 patients. In addition to the IID TFC changes, there were subchondral cysts in the adjacent lunate and triquetrum, and osteoarthritic changes in the ulnocarpal/radioulnar joint. On MR images, there was a complete tear of the TFC, which became irregular with increased signal intensity, with complete loss of the articular cartilage along the ulnar side of the proximal lunate with cystic changes, indicating subchondral cyst formation. There was joint effusion in the DRUJ with subchondral cyst formation and osteophyte formation, as shown on the PD FS images (Fig. 10).

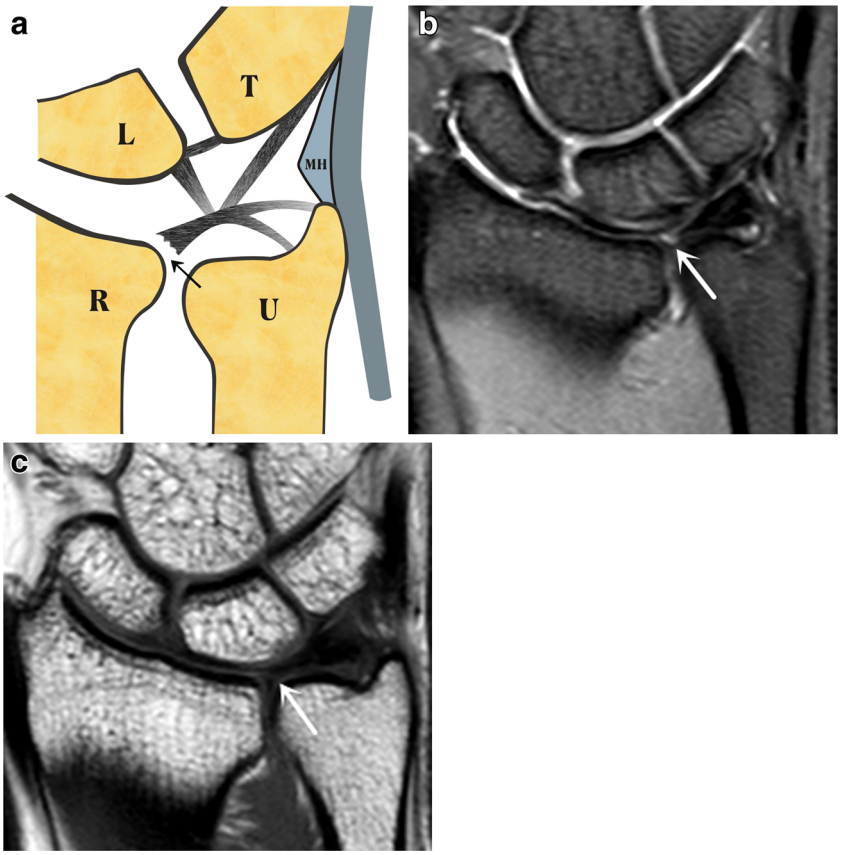

Fig. 4 Class ID: radial avulsion. **a** Illustration of Palmer ID injury showed the avulsion of the TFCC from the radial attachment. **b, c** A 30-year-old woman with a wrist injury. **b** Coronal PD FS image and **c** coronal T1-weighted image showed discontinuity of the TFC with abnormal hypersignal intensity at the radial attachment (*arrow*)

TFCC injuries not included in the Palmer classification and their MR features

Horizontal tear of the articular disk

There were 4 cases with horizontal tear of the TFC. The tear occurred along the transverse plane of the TFC in the horizontal direction based on the anatomical position of the wrist (Fig. 11). This tear was different from the IA Palmer injury that occurred in the sagittal direction. On PD FS weighted images, it was demonstrated as horizontal oriented linear hypersignal intensity in the middle of the TFC disk, which paralleled the superior and inferior surfaces (Fig. 11).

Capsular TFC detachment

Class IF indicated volar capsular TFC detachment and was found in 1 patient. This injury mainly showed the separation between the volar side edges of the TFC with the volar side joint capsule. On sagittal PD FS weighted images, there was hypersignal intensity between the volar edge of the articular disk and the joint capsule (Fig. 12).

Class IC described the distal detachment of the TFC from the volar side joint capsule (Fig. 3).

Class IG indicated dorsal capsular TFC detachment and was found in 8 patients. It was characterized by the partial or complete detachment of the dorsal capsule from the TFC (Fig.

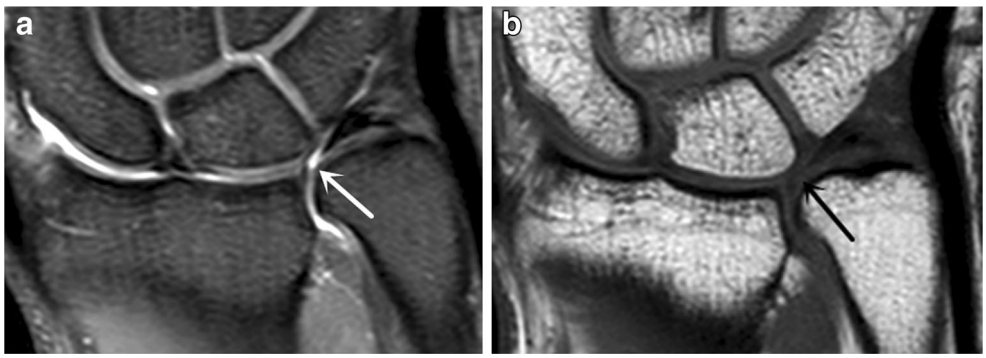

Fig. 5 Class ID: radial avulsion. **a**, **b** A 33-year-old woman with a wrist injury, which we misinterpreted as central perforation; the surgical result was proven to be radial avulsion of the TFC. **a** Coronal PD FS image and **b** coronal T1-weighted image showed the abnormal high signal intensity (*arrow*) between the radial attachment of the TFCC and the hyaline cartilage of the distal radius

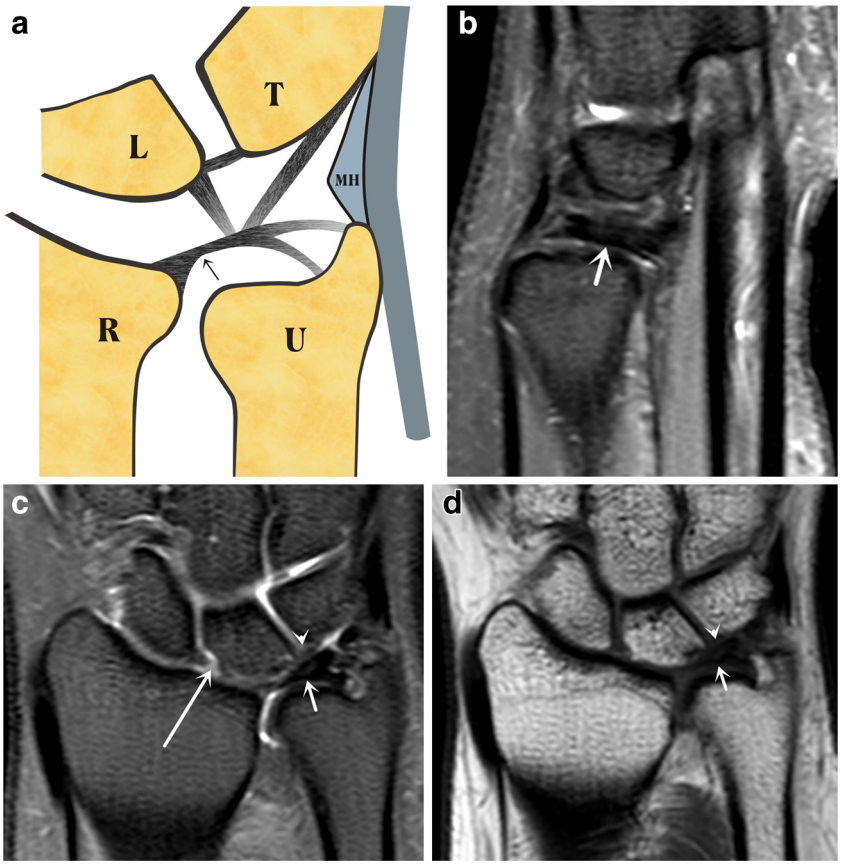

Fig. 6 Class IIA: TFC wear. **a** Illustration of Palmer IIA injury showed the wearing or thinning of the TFC. **b–d** A 44-year-old woman with wrist pain. **b** Sagittal, **c** coronal PD FS images and **d** coronal T1-weighted image showed intermediate signal intensity (*arrow*) in the normal low signal TFC, which was a direct result of the wearing of the central portion of the TFCC. This injury was best visualized on the PD FS images. In this patient, the intact lunotriquetral ligament (*arrowhead*) could be observed. In addition, a scapholunate ligament tear could be observed in this case (*long arrow* in **c**)

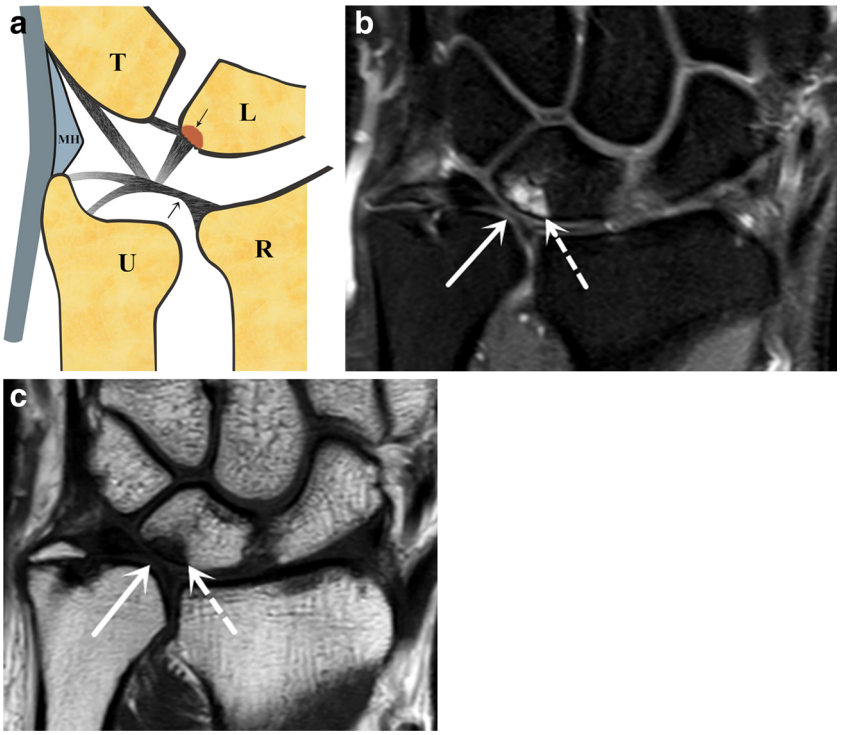

Fig. 7 Class IIB: TFC wear and chondromalacia. **a** Illustration of Palmer IIB showed thinning of the TFC proper and the subchondral cyst and cartilage changes of the adjacent lunate. **b**, **c** A 51-year-old man with wrist pain. **b** Coronal PD FS image and **c** coronal T1-weighted image showed intermediate signal intensity within the thinning TFC (*arrow*), the subchondral cyst and marrow edema of the adjacent lunate and focally thinning cartilage (*dashed arrow*)

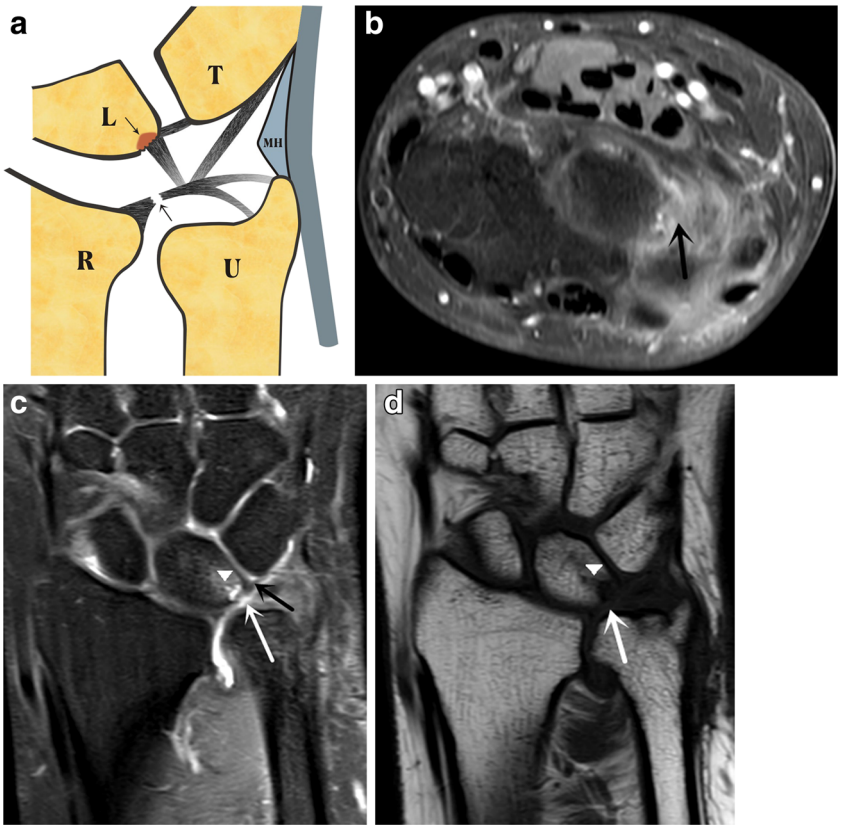

Fig. 8 Class IIC: TFC perforation and chondromalacia. **a** Schematic drawing of Palmer IIC injury. **b–d** A 43-year-old woman with a wrist injury. **b** Axial, **c** coronal PD FS images, and **d** coronal T1-weighted image showed the TFC perforation, which was shown as increased signal intensity within the thinning TFC (*black arrow* in **b**, *white arrow* in **c** and **d**), and it could be well evaluated on the PD FS images. There was effusion in the DRUJ, subchondral cyst, and edema of the adjacent lunate (*white arrowhead* in **c** and **d**), and focally thinning cartilage. The lunotriquetral ligament was intact and showed as a band of low signal intensity (*black arrow* in **c**)

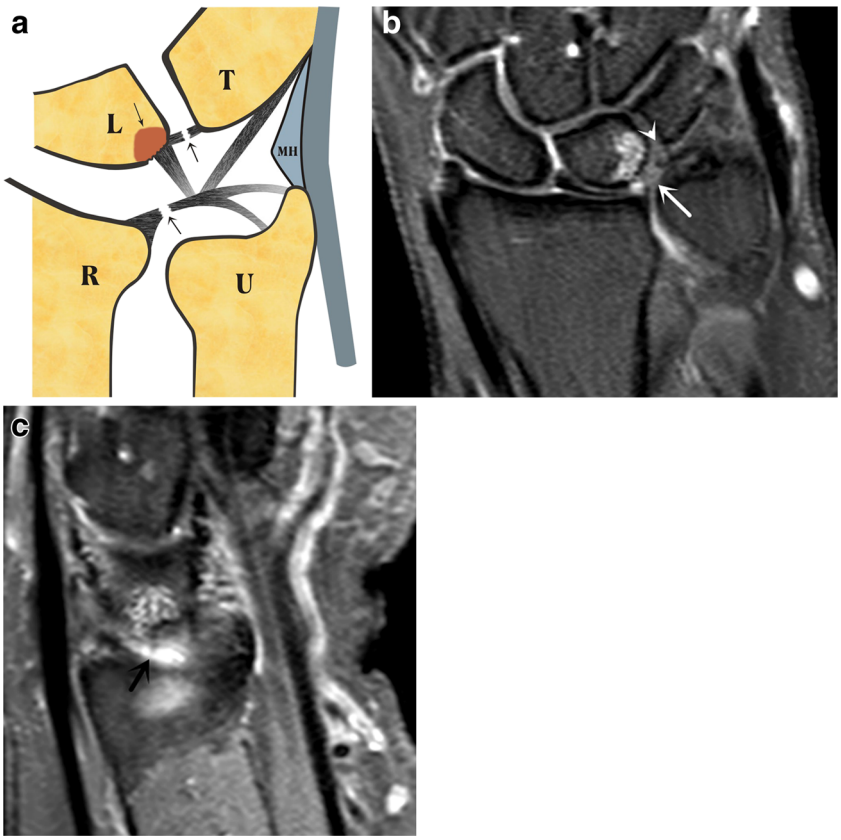

Fig. 9 Class IID: TFC perforation, chondromalacia, and lunotriquetral ligament disruption. **a** Illustration of Palmer IID injury. **b**, **c** A 79-year-old woman with a wrist injury. **b** Coronal PD FS image and **c** sagittal PD FS image showed the discontinuity and increased signal intensity of the TFC (*arrow*), subchondral cyst and edema of the adjacent lunate, and the focally thinning cartilage and the increased signal intensity in the obscure lunotriquetral ligament (*arrowhead* in **b**)

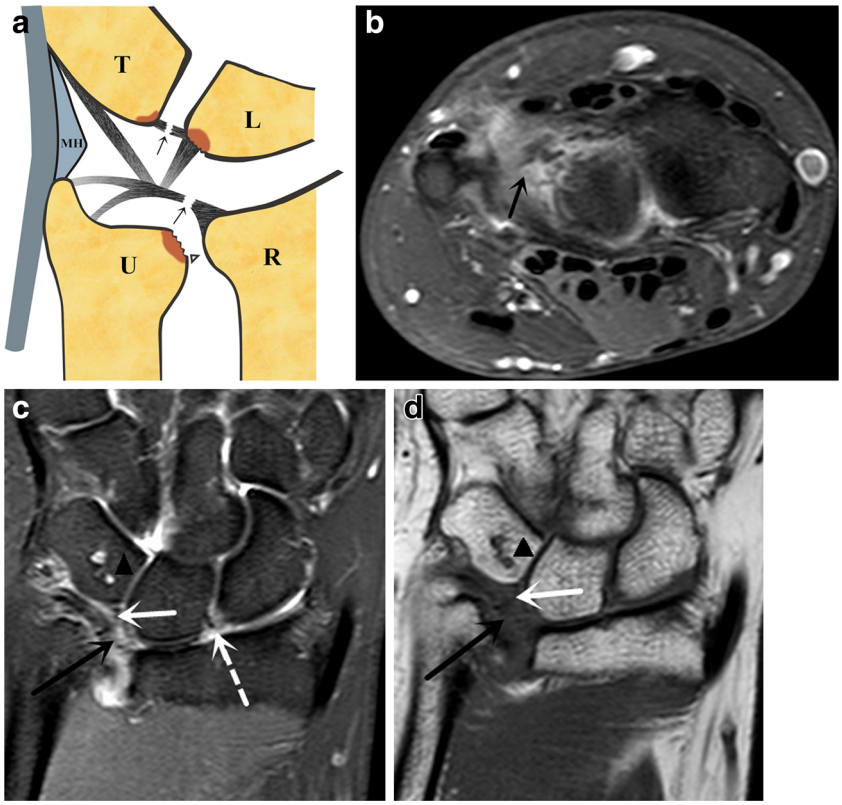

Fig. 10 Class IIE: TFC perforation, chondromalacia, lunotriquetral ligament perforation, and ulnocarpal/radioulnar arthritis. **a** Schematic drawing of Palmer IIE injuries. **b–d** A 48-year-old woman with wrist injury. **b** Axial, **c** coronal PD FS-weighted images, and **d** coronal T1-weighted image showed high signal intensity within the thinning and obscure TFC (*black arrow*), the effusion in the DRUJ, the cyst of the adjacent triquetrum (**c**, **d** *black arrowhead*), the loss of focal cartilage, high signal intensity in PD images of the obscure lunotriquetral ligament (*white arrow* in **c** and **d**). In addition, a scapholunate ligament tear could also be observed in this case (*dashed arrow* in **c**)

13). On PD FS images, the articular disk was separated from the dorsal joint capsule by an area of high signal intensity (Fig. 13).

Class IH indicated dorsal capsular detachment from the triquetral insertion and was found in 3 patients. On MR images, this lesion could be best seen on sagittal PD FS images as discontinuity of the dorsal joint capsule with an area of hypersignal intensity between the distal joint capsule and the dorsal aspect of the triquetrum (Fig. 14).

Class II indicated dorsal capsular TFC detachment and detachment from the triquetral insertion and was found in 1 patient. This type of injury was best evaluated in the sagittal plane. There was a linear hypersignal intensity gap between the dorsal joint capsule and the dorsal aspect of the TFC and detachment of the dorsal joint capsule from the dorsal aspect of the triquetrum (Fig. 15).

Discussion

Palmer classification (listed in Table 1) has been widely used by hand surgeons and can help to identify the mechanism of injuries and direct clinical management [15, 16]. However, there were 17 patients whose injuries could not be classified by using the Palmer classification in our study. We feel that the Palmer classification cannot cover all TFCC injuries, which is

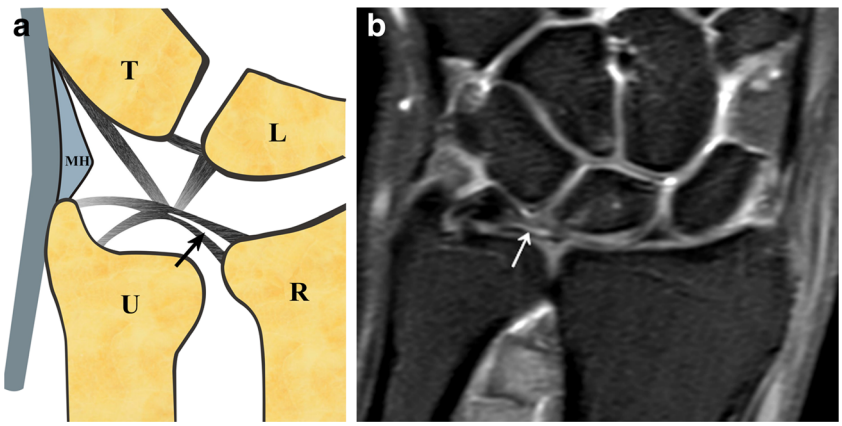

Fig. 11 Horizontal tear of the articular disk. **a** Schematic drawing of the horizontal tear of the articular disk showed the horizontal tear within the TFC (*arrow*), which was different from the IA Palmer injury. This tear does not extend into the joint surface. **b** A 59-year-old woman with wrist pain after injury. On coronal PD FS weighted images, there was linear hypersignal intensity within the TFC (*arrow*)

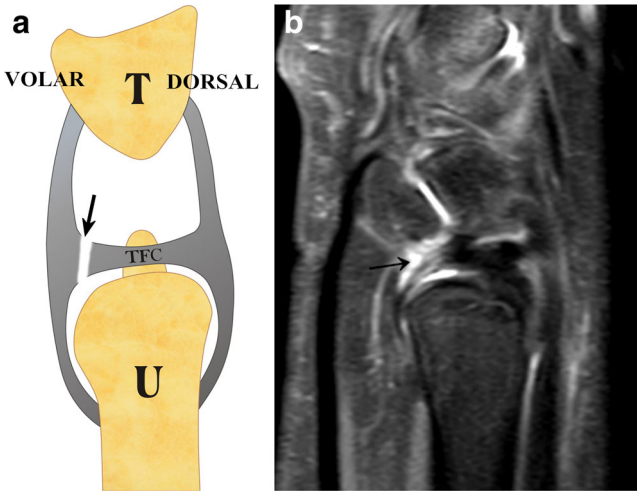

Fig. 12 Volar capsular TFC detachment. **a** Schematic drawing of volar capsular detachment. **b** A 15-year-old girl with a right wrist injury. Sagittal PD FS image showed the high signal intensity in the insertion of the volar edge of the articular disk (*arrow*), which was different from IC Palmer injuries

in line with what has been reported by other authors [17–20]. They all stated that not all TFCC injuries could fit exactly into the Palmer classification. Therefore, we propose a modified Palmer classification, adding the capsular injuries and horizontal tear of the articular disk into the classification of TFCC injuries (Table 2).

Sachar [21] found that the central perforation of TFC was the most common traumatic subtype. However, in our study there were only 9 people with central perforation. The most common traumatic injury of the TFC was ulnar detachment of the TFC. There were 25 patients with ulnar detachment of the TFC. This discrepancy may be due to the different patient population, as our patient populations were selected because they had all undergone surgery. The central perforation of the

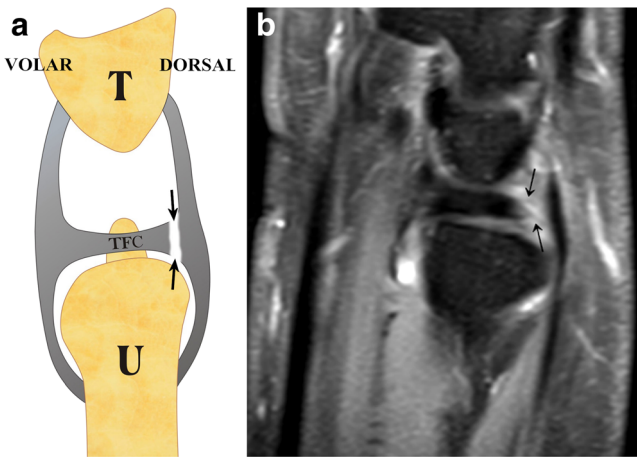

Fig. 13 Dorsal capsular TFC detachment. **a** Sagittal schematic drawing demonstrated the detachment of TFC from the dorsal capsule (*arrow*). **b** A 36-year-old woman with a left wrist injury. The sagittal PD FS image showed the complete detachment of the dorsal aspect of the articular disk from the dorsal aspect of the capsule (*arrow*)

TFC showed a slit-like area of high signal intensity on PD FS images and traveled in a sagittal direction, although it usually required treatment with debridement because the central perforation occurred in the avascular portion of the TFC and it would not heal itself [22]. In our patient population, some of the patients with central perforation of the TFC may not undergo surgery, whereas most of the patients with ulnar attachment tear do have surgery repair. The relatively small sample size may also play a role.

In our study, among 25 patients with ulnar avulsion, 24 people showed only the increased signal intensity in the attachment of the ulna. The ulnar attachment of TFCC cannot be clearly identified owing to the diffuse increased signal intensity in this region. One patient had fracture of the base of the ulnar styloid, which confirmed the statement that these tears may be associated with a fracture through the base of the ulnar styloid, as reported previously [15, 16, 23]. As the TFCC is one of the major stabilizers of the DRUJ, this type of lesion can often be associated with the instability of the DRUJ, and it often needs surgical repair [24]. There were 3 patients with distal TFC avulsion, 1 of the patients also had a Colles fracture whereas the other had fractures of the scaphoid and triquetrum and multiple ligament injuries including the scapholunate ligament and the lunotriquetral ligament. These findings confirmed what Skalski et al. reported, that type IC was uncommon and usually associated with multiple wrist injuries [17]. However, the detail still needed to be further investigated because of the small sample size in this research. In this study, we found that the distal avulsion of the TFC could be better recognized on sagittal PD FS images. This type of injury can result in ulnocarpal instability with palmar displacement of the carpus in relation to the radius and/or ulnar head, and an open or arthroscopic repair can be performed [24].

Finally, there were 13 patients with radial avulsion (type ID lesion) and their MR image features needed to be carefully examined. This type of injury needs to be differentiated from type IA, central perforation. In our study, 2 patients with type ID lesion were misinterpreted as having central perforation (type IA lesion) by both reviewers independently, whereas the surgical results proved radial avulsion. The key feature of the type ID lesion, radial avulsion, is the detachment of the TFC from the distal radial articular cartilage. The central disk, the TFC itself, is intact whereas the type IA lesion, central perforation, is a tear of the TFC. In a type IA lesion, a piece of TFC should still be attached to the sigmoid notch. Because the articular disk is avascular, there is little chance for healing after repair; thus, the central perforation is generally not amenable to direct repair, and needs arthroscopic debridement, whereas the radial avulsion may need arthroscopic reattachment. In radial avulsion, the abnormal high signal intensity on PD FS images was closer to the radial side between the radial attachment of the TFCC and the hyaline cartilage of the distal radius, whereas the slit-like area of high signal intensity

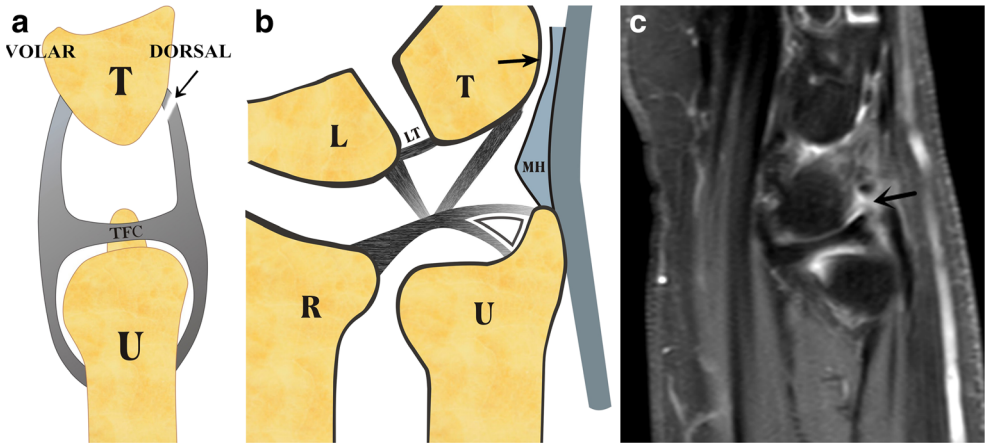

Fig. 14 Dorsal capsular detachment from the triquetral insertion. **a**, **b** Sagittal and coronal drawing illustrated the distal detachment of the dorsal capsule in its insertion in the dorsal aspect of the triquetrum (*arrow*). **c** A 60-year-old woman with a left wrist injury. On a sagittal PD FS image, the distal detachment at the dorsal triquetrum edge showed irregular and discontinued structure with an area of high signal intensity at the distal insertion of the triquetrum (*arrow*)

of the central perforation was confined to the TFC disk. In a further study, we will collect more cases to investigate the discrepancy between the MRI and the surgical results, and provide practical diagnostic skills for distinguishing between types IA and ID.

In this study, there were 17 patients with degenerative injuries (class II). Among them, 11 had ulnar impaction or abutment syndrome and 6 had osteoarthritis resulting from the normal aging process, which corresponded to the literature, which indicated that class II lesions may be associated with chronic loading of the ulnar wrist, ulnar impaction or abutment syndrome and positive ulnar variance [16, 17, 25, 26]. In our study, the average age of patients with degenerative lesions was 50 years, indicating that class II lesions were more likely to occur in an older population, which again was in line with the literature [27]. What needed to be specified was that the central perforation in class IIC was different from that in class I, which often showed a slit-like tear. Cody et al. found that in degenerative injuries, the perforation of TFC tended to be more ovoid and was located more toward the ulnar aspect of the disk [16].

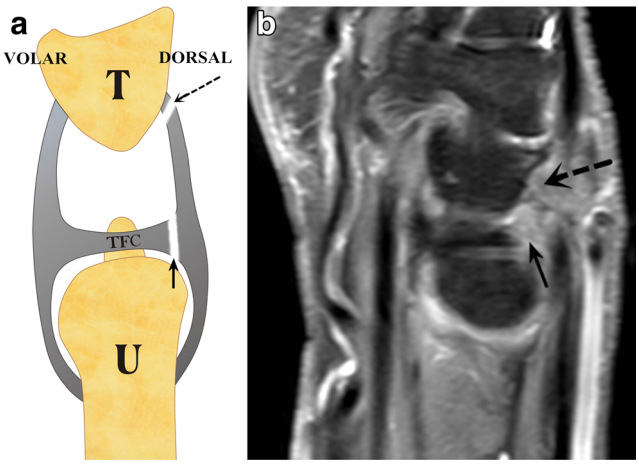

Fig. 15 Dorsal capsular TFC detachment and detachment from the triquetral insertion. **a** Illustration of a combined injury: dorsal capsular detachment (*arrow*) coupled with the detachment in the insertion into the dorsal edge of the triquetrum (*dashed arrow*). **b** A 68-year-old woman with a right wrist injury. The sagittal PD FS image showed the detachment in the dorsal capsule (*arrow*) and the insertion into the dorsal edge of the triquetrum (*dashed arrow*) with high signal intensity

We found that in non-Palmer injuries, the dorsal capsular detachment was more common than in other types, even compared with the IC Palmer injury. Moreover, this type of injury can lead to the dorsal displacement of the ulna and the disability of the wrist and usually requires external fixation. If the conservative treatment failed, then those patients usually needed surgical treatment. However, further study is necessary because of the small sample in our study.

This study carries several limitations. Owing to the small sample size, the common and uncommon traumatic subtype should be further studied. Because we want to present all surgically proven cases, the patient population is biased by the inclusion criteria. Many more TFCC injury patients have to be excluded from our study owing to the lack of surgical approval. The literature agreed that conventional MR imaging could detect moderate and severe cases of class IIA and IIB [15, 17]. MR arthrography with contrast medium injected into the distal radioulnar joint could increase the sensitivity of detecting subtle TFCC lesions. In our study, without MR arthrography (which could not be performed because of the invasiveness and the increased pain for patients), we carried out only MRI as a non-invasive method, which made our study somewhat incomplete. MR arthrography will be included in future studies.

Conclusions

Using high-resolution 3-T MRI, we have not only found all the TFCC injuries described in the Palmer classification, additional injury types were found in this study, including horizontal tear of the TFC and capsular TFC detachment. We propose the modified Palmer classification and add injury types that were not included in the original Palmer classification.

Acknowledgements This study was funded by the National Natural Science Foundation of China (grant number 81371515), the Beijing Natural Science Foundation of China (grant number 7142075), the Capital Medical Development and Scientific Research Fund of China (grant number 2016-2-1122).

Compliance with ethical standards

Conflicts of interest The authors declare that they have no conflict of interest.

Ethical approval All procedures performed in studies involving human participants were in accordance with the ethical standards of the institutional and/or national research committee and with the 1964 Declaration of Helsinki and its later amendments or comparable ethical standards.

Informed consent Informed consent was obtained from all individual participants included in the study.

References

1. Nakamura T, Yabe Y, Horiuchi Y. Functional anatomy of the triangular fibrocartilage complex. J Hand Surg Br. 1996;21(5):581–6. doi:10.1016/S0266-7681(96)80135-5.
2. Nakamura T, Yabe Y. Histological anatomy of the triangular fibrocartilage complex of the human wrist. Ann Anat. 2000;182(6):567–72. doi:10.1016/S0940-9602(00)80106-5.
3. Cerezal L, de Dios B-MJ, Canga A, et al. MR and CT arthrography of the wrist. Semin Musculoskelet Radiol. 2012;16(1):27–41. doi:10.1055/s-0032-1304299.
4. Cerezal L, Abascal F, García-Valtuille R, Del Piñal F. Wrist MR arthrography: how, why, when. Radiol Clin N Am. 2005;43(4):709–31. doi:10.1016/j.rcl.2005.02.004.
5. Ahn AK, Chang D, Plate AM. Triangular fibrocartilage complex tears: a review. Bull NYU Hosp Jt Dis. 2006;64(3-4):114–8.
6. Palmer AK, Werner FW. The triangular fibrocartilage complex of the wrist—anatomy and function. J Hand Surg Am. 1981;6(2):153–62.
7. Linscheid RL. Biomechanics of the distal radioulnar joint. Clin Orthop Relat Res. 1992;275:46–55. doi:10.1097/00003086-199202000-00008.
8. Fotiadou A, Patel A, Morgan T, Karantanas AH. Wrist injuries in young adults: the diagnostic impact of CT and MRI. Eur J Radiol. 2011;77(2):235–9. doi:10.1016/j.ejrad.2010.05.011.
9. Clavero JA, Alomar X, Monill JM, et al. MR imaging of ligament and tendon injuries of the fingers. Radiographics. 2002;22(2):237–56. doi:10.1148/radiographics.22.2.g02mr11237.
10. Jeantroux J, Becce F, Guerini H, Montalvan B, Le Viet D, Drapé JL. Athletic injuries of the extensor carpi ulnaris subsheath: MRI findings and utility of gadolinium-enhanced fat-saturated T1-weighted sequences with wrist pronation and supination. Eur Radiol. 2011;21(1):160–6. doi:10.1007/s00330-010-1887-3.
11. Watanabe A, Souza F, Vezeridis PS, Blazar P, Yoshioka H. Ulnar-sided wrist pain. II. Clinical imaging and treatment. Skeletal Radiol. 2010;39(9):837–57. doi:10.1007/s00256-009-0842-3.
12. Anderson ML, Skinner JA, Felmlee JP, Berger RA, Amrami KK. Diagnostic comparison of 1.5 Tesla and 3.0 Tesla preoperative MRI of the wrist in patients with ulnar-sided wrist pain. J Hand Surg Am. 2008;33(7):1153–9. doi:10.1016/j.jhsa.2008.02.028.
13. Potter HG, Asnis-Ernberg L, Weiland AJ, Hotchkiss RN, Peterson MG, McCormack RR Jr. The utility of high-resolution magnetic resonance imaging in the evaluation of the triangular fibrocartilage complex of the wrist. J Bone Joint Surg Am. 1997;79(11):1675–84. doi:10.2106/00004623-199711000-00009.
14. Palmer AK. Triangular fibrocartilage complex lesions: a classification. J Hand Surg Am. 1989;14(4):594–606. doi:10.1016/0363-5023(89)90174-3.
15. Oneson SR, Scales LM, Timins ME, Erickson SJ, Chamoy L. MR imaging interpretation of the Palmer classification of triangular fibrocartilage complex lesions. Radiographics. 1996;16(1):97–106. doi:10.1148/radiographics.16.1.97.
16. Cody ME, Nakamura DT, Small KM, Yoshioka H. MR imaging of the triangular fibrocartilage complex. Magn Reson Imaging Clin N Am. 2015;23(3):393–403. doi:10.1016/j.mric.2015.04.001.
17. Skalski MR, White EA, Patel DB, Schein AJ, RiveraMelo H, Matcuk GR Jr. The traumatized TFCC: an illustrated review of the anatomy and injury patterns of the triangular fibrocartilage complex. Curr Probl Diagn Radiol. 2016;45(1):39–50. doi:10.1067/j.cpradiol.2015.05.004.
18. Daunt N. Magnetic resonance imaging of the wrist: anatomy and pathology of interosseous ligaments and the triangular fibrocartilage complex. Curr Probl Diagn Radiol. 2002;31(4):158–76. doi:10.1067/cdr.2002.125780.
19. Van Schoonhoven J. Arthroscopy of the wrist and hand. Oper Orthop Traumatol. 2014;26(6):537–8. doi:10.1007/s00064-014-0355-7.
20. Estrella EP, Hung L-K, Ho P-C, Tse WL. Arthroscopic repair of triangular fibrocartilage complex tears. Arthroscopy. 2007;23(7):729–737, 737.e1. doi:10.1016/j.arthro.2007.01.026.
21. Sachar K. Ulnar-sided wrist pain: evolution and treatment of triangular fibrocartilage complex tears, ulnocarpal impaction syndrome, and lunotriquetral ligament tears. J Hand Surg Am. 2012;37(7):1489–500. doi:10.1016/j.jhsa.2012.04.036.
22. Zanetti M, Linkous D, Gilula LA, Hodler J. Characteristics of triangular fibrocartilage defects in symptomatic and contralateral asymptomatic wrists. Radiology. 2000;216(3):840–5. doi:10.1148/radiology.216.3.r00se06840.
23. Hobby JL, Tom BD, Bearcroft PW, Dixon AK. Magnetic resonance imaging of the wrist: diagnostic performance statistics. Clin Radiol. 2001;56(1):50–7. doi:10.1053/crad.2000.0571.
24. Von Borstel D, Wang M, Small K, Nozaki T, Yoshioka H. High-resolution 3T MR imaging of the triangular fibrocartilage complex. Magn Reson Med Sci. 2017;16:3–15. doi:10.2463/mrms.rev.2016-0011.
25. Cerezal L, del Piñal F, Abascal F, Garcia-Valtuille R, Pereda T, Canga A. Imaging findings in ulnar-sided wrist impaction syndromes. Radiographics. 2002;22(1):105–21. doi:10.1148/radiographics.22.1.g02ja01105.
26. Woitzik E, de Grauuw C, Easter B. Ulnar impaction syndrome: a case series investigating the appropriate diagnosis, management, and postoperative considerations. J Can Chiropr Assoc. 2014;58(4):401–12.
27. Mikić ZD. Age changes in the triangular fibrocartilage of the wrist joint. J Anat. 1978;126(Pt2):367–84.